Available online at www.sciencedirect.com
ScienceDirect
Journal of the European Ceramic Society 30 (2010) 1035–1042
www.elsevier.com/locate/jeurceramsoc

Fabrication and properties of ZrB_2–SiC–BN machinable ceramics

Haitang Wu [a,b], Weigang Zhang [a,*]

[a] State Key Laboratory of Multi-Phase Complex Systems, Institute of Process Engineering, Chinese Academy of Sciences, Beijing 100190, PR China
[b] Graduate University of Chinese Academy of Sciences, Beijing 100049, PR China

Received 16 April 2009; received in revised form 5 September 2009; accepted 22 September 2009
Available online 29 October 2009

Abstract

ZrB_2–SiC–BN ceramics were fabricated by hot-pressing under argon at 1800 °C and 23 MPa pressure. The microstructure, mechanical and oxidation resistance properties of the composite were investigated. The flexural strength and fracture toughness of ZrB_2–SiC–BN (40 vol%ZrB_2–25 vol%SiC–35 vol%BN) composite were 378 MPa and 4.1 MPa $m^{1/2}$, respectively. The former increased by 34% and the latter decreased by 15% compared to those of the conventional ZrB_2–SiC (80 vol%ZrB_2–20 vol%SiC). Noticeably, the hardness decreased tremendously by about 67% and the machinability improved noticeably compared to the relative property of the ZrB_2–SiC ceramic. The anisothermal and isothermal oxidation behaviors of ZrB_2–SiC–BN composites from 1100 to 1500 °C in air atmosphere showed that the weight gain of the 80 vol%ZrB_2–20 vol%SiC and 43.1 vol%ZrB_2–26.9 vol%SiC–30 vol%BN composites after oxidation at 1500 °C for 5 h were 0.0714 and 0.0268 g/cm^2, respectively, which indicates that the addition of the BN enhances oxidation resistance of ZrB_2–SiC composite. The improved oxidation resistance is attributed to the formation of ample liquid borosilicate film below 1300 °C and a compact film of zirconium silicate above 1300 °C. The formed borosilicate and zirconium silicate on the surface of ZrB_2–SiC–BN ceramics act as an effective barriers for further diffusion of oxygen into the fresh interface of ZrB_2–SiC–BN.

Keywords: Zirconium diboride; Boron nitride; Oxidation resistance; Mechanical properties; Machinability

1. Introduction

Ultra-high temperature ceramics (UHTCs) including refractory diborides and carbides, such as ZrB_2, HfB_2, ZrC, HfC and TaC, are considered as the most promising materials for the application in critical thermal protection systems and other components of future hypersonic aircraft or re-entry vehicles. Compared to the single-phase monolithic UHTC, ZrB_2–SiC composite is of particular interest because of its striking property combination of high melting point, resistance to ablation/oxidation at high temperatures, high electrical and thermal conductivity and thermal-shock resistance, which makes it an attractive potential candidate for aerospace applications.[1–5]

Machining is an inevitable requirement for flexible use of advanced ceramics, especially when the complex and precision components of structural ceramics are involved. The use of diamond tools and some special processing technologies such as laser machining and ultrasonic machining are often inefficient and costly (machining cost usually accounts for 70–90% of the total cost) though those processes make some hard ceramics materials machinable.[6] Electrical discharge machining is another promising technology to machine ceramic components of complex shape with high-dimensional accuracy and low surface roughness. Except for the inefficiency, electrical discharge machining requires a material resistance and can only machine components of small size.[7] Comparatively, traditional mechanical machining is of both cost-effective and time-efficient. However, the extremely high strength and hardness of ZrB_2–SiC due to the coexistence of strong covalent and metallic bond make mechanical machining very difficult or even impossible. This prevents the material from wide application. In recent years, attempts have been made to improve the machinability of ceramic materials by introducing in the matrix weak interfaces material, such as mica, h-BN, graphite, pores, rare-earth phosphates and Ti_3SiC_2 analogous compounds, to facilitate crack deflection during machining.[8] Among those materials, h-

* Corresponding author at: State Key Laboratory of Multi-Phase Complex Systems, Institute of Process Engineering, Chinese Academy of Sciences, Beijing 100190, PR China. Tel.: +86 10 62520135; fax: +86 10 62520135.
E-mail address: wgzhang@home.ipe.ac.cn (W. Zhang).

0955-2219/$ – see front matter © 2009 Elsevier Ltd. All rights reserved.
doi:10.1016/j.jeurceramsoc.2009.09.022

BN, which exhibits high thermal conductivity and high melting point, is regarded as a suitable and effective interface material since the cleavage plane of h-BN facilitates crack propagation and decreases the cutting resistance during machining.[9–12] Besides these, the similar crystal structures of BN and ZrB_2 ensure the good chemical compatibility between them. Therefore, ZrB_2–SiC–BN system may be a good candidate material for high temperature ceramics with excellent machinability and mechanical properties.

In this paper, the fabrication of a machinable ZrB_2–SiC–BN composite with excellent mechanics properties and oxidation resistance properties was reported. Influences of BN content on the hardness, fracture toughness, flexural strength and oxidation resistance property of the composite were investigated. The oxidation resistance properties tested at from 1100 to 1500 °C were reported here. As the operative temperature for UHTC materials is in excess of 2000 °C, composition performing better than others at 1500 °C may not necessarily apply to higher temperature ranges. The oxidation resistance of this composite and the optimization of the composition at more than 2000 °C are also under investigation.

2. Experimental procedure

2.1. Samples preparation

Four kinds of ZrB_2–SiC–BN composites with various powder compositions (vol%) were prepared (see Table 1).

Commercially available ZrB_2 powder (>99% purity, an average particle size of 3 μm, Northwest Institute for non-ferrous metal research, China), SiC powder (>98.5% purity, an average particle size of 1.5 μm, Weifang Kaihua Micro-powder Co., Ltd., China) and h-BN powder (>99% purity, 4 μm, Chem Factory, Beijing, China) were used. Powders were mixed and ball-milled for 12 h in a polyethylene bottle charged with ethanol using ZrO_2 balls. Solvent was then removed using a rotary evaporator. The dried powder mixtures were sintered by hot-pressing in an argon atmosphere at 1800 °C and 23 MPa pressure for 1 h in graphite dies coated with pyrolytic BN.

2.2. Characterization

Bulk density and theoretical density were measured and assessed by the Archimedes method and the rule-of-mixture, respectively. Phase composition was identified by X-ray diffraction (XRD; Rigaku, Dmax-rb) using Cu K_α radiation. The microstructure was characterized by field emission scanning electron microscopy (SEM; S4700, Hitachi, Tokyo, Japan) and chemical compositions were evaluated by energy-dispersive X-ray spectroscopy (EDS; Phoenix, EDAX, Mahwah, NJ). Flexural strength was tested in a three-point configuration (3 mm × 4 mm × 36 mm chamfered bars), with a 30 mm span and a crosshead speed of 0.5 mm/min. Fracture toughness was evaluated by a single-edge notched beam test with a 16 mm span and a crosshead speed of 0.05 mm/min using 2 mm × 4 mm × 22 mm test bars. Hardness was determined by Vickers indentation (Model HVS-5, Laizhou Huayin Experimental Instrument Limited Company, China) using a diamond indenter with a load of 98 N for 15 s.

Table 1
Composition of the prepared composite samples.

Sample	ZrB_2	SiC	BN	ZrB_2:SiC:BN
ZS0	80%	20%	0%	4:1:0
ZS1	56%	14%	30%	4:1:2.14
ZS2	43.1%	26.9%	30%	4:2.5:2.78
ZS3	40%	25%	35%	4:2.5:3.5

2.3. Oxidation tests

Specimens were cleaned in an ultrasonic bath in acetone before oxidation. The isothermal static oxidation tests were conducted in an electrical furnace at temperatures of 1100, 1300 and 1500 °C in air with interruptions in the tests in order to measure weight (to an accuracy of 0.0001 g) change at fixed times. The specific weight change was calculated according to the mass change per surface area.

The oxidation resistance of specimen was also tested by a Netzsch STA449C thermogravimetric analyzer. The mass changes were followed at a rate of 5°/min up to 1500 °C with an 2 h isothermal hold in a flowing air (50 ml/min).

3. Results and discussion

3.1. Mechanical properties and machinability

Fig. 1 shows the XRD results of sintered ceramics containing various contents of BN. All samples contained the initial phases of ZrB_2, SiC and BN, except the sample ZS0 in which no BN existed. No new phase was formed during hot-pressing and sintering. Therefore, no chemical reactions occurred under the experimental condition, which benefits the formation of weak interfaces between the boundaries of ZrB_2, SiC and BN grains.

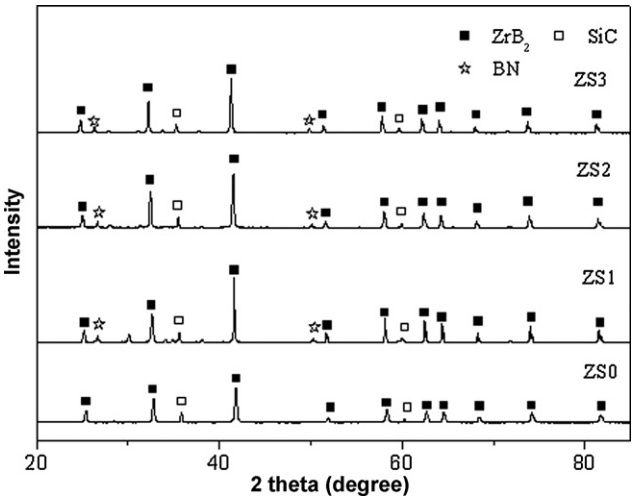

Fig. 1. XRD patterns of ZrB_2 based composites.

Table 2
Density and mechanical properties of ZrB_2–SiC and ZrB_2–SiC–BN composites.

Sample	Composition (vol%)	Apparent density (g/cm^3)	Relative density (%)	Flexural strength (MPa)	Fracture toughness ($MPa\,m^{1/2}$)	Vickers hardness (GPa)
ZS0	80%ZrB_2 + 20% SiC	5.129	93.0	281	4.8	15.9
ZS1	56%ZrB_2 + 14%SiC + 30%BN	4.102	90.3	301	3.5	5.9
ZS2	43.1%ZrB_2 + 26.9%SiC + 30%BN	3.775	90.6	317	3.7	5.6
ZS3	40%ZrB_2 + 25%SiC + 35%BN	3.735	92.6	378	4.1	52

Results of density and mechanical properties are listed in Table 2. An increase in the flexural strength of ZrB_2–SiC composites doped BN was found compared to that of ZrB_2–SiC composite without BN. This mainly results from the fact that the h-BN crystals were homogeneously dispersed around the matrix grains of ZrB_2 and SiC during sintering (as shown in Fig. 2), which limits the grain growth and improves their flexural strengths.

It is assumed that the soft h-BN particles with layered-structures could relax stress and absorb energy at the crack tip through microcracking or crack-particle interactions, then prevent the main crack from extending which should be propitious to improve fracture toughness.[13–15] However, compared to ZrB_2–SiC, the fracture toughnesses of all ZrB_2–SiC–BN composites decreased in the study.

On the other hand, Table 2 shows that the hardness of the ZrB_2–SiC–BN composite decreased greatly with 30 vol%BN additive compared to pure ZrB_2–SiC. Hardness is an important indicator for ceramic machinability. Generally, a lower hardness leads to an improved machinability. Fig. 3 shows a hole made by cemented carbide drills on the ZS2 specimen. It can be seen that the ZrB_2–SiC–BN composite is successfully machined. However, due to high hardness, the ZS0 specimen without BN additive cannot be machined using such drills. As stated above, the layered structure of BN resulting in a weak interface at the ZrB_2–SiC–BN grain boundaries is the main reason for the improvement of the machinability, which can enhance the crack deflection and avoid the catastrophic failure of the material during drilling.

Fig. 4 shows the fracture surface of specimens for a test of fracture toughness. It can be seen that abnormal grain growth occurs in the ZS0 specimen with a main fracture model of transgranular fracture. For the ZS1, ZS2 and ZS3 specimens, fractures propagate parallel to the layer crystals because BN grains possess a layered crystal structure and are readily delaminated due to its low cleavage energy. Crack deflections, branching and blunting during machining of layered crystal BN are beneficial to prevent macroscopic fractures from propagation beyond the local cutting area, which lead to fracture modes dominated by the intergranular fracture. This phenomenon confirms the formation of weak ZrB_2–SiC–BN interfaces by the addition of BN and is the main reason for the improved machinability of this composite.

3.2. Oxidation resistance

3.2.1. Thermal gravimetric analysis (TGA)

Fig. 5 shows the mass changes of the four specimens. It is shown that there is a similar tendency as the temperature below

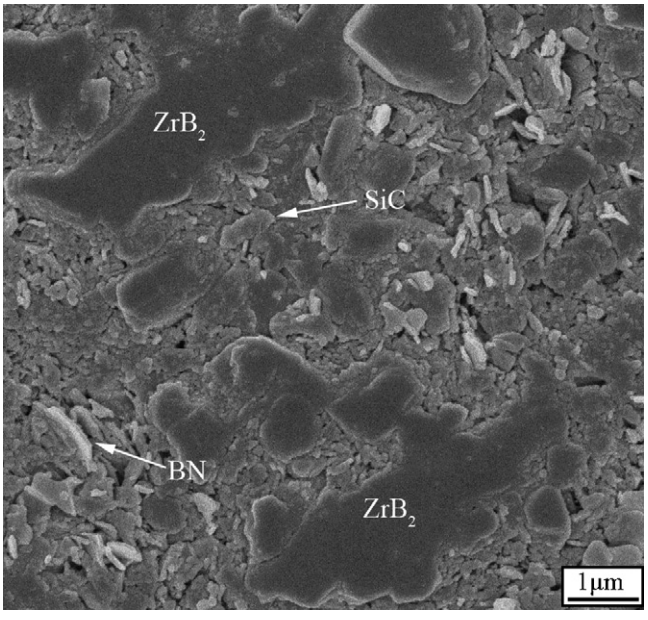

Fig. 2. Cross-sectional SEM micrograph from polished section of ZS2 composite.

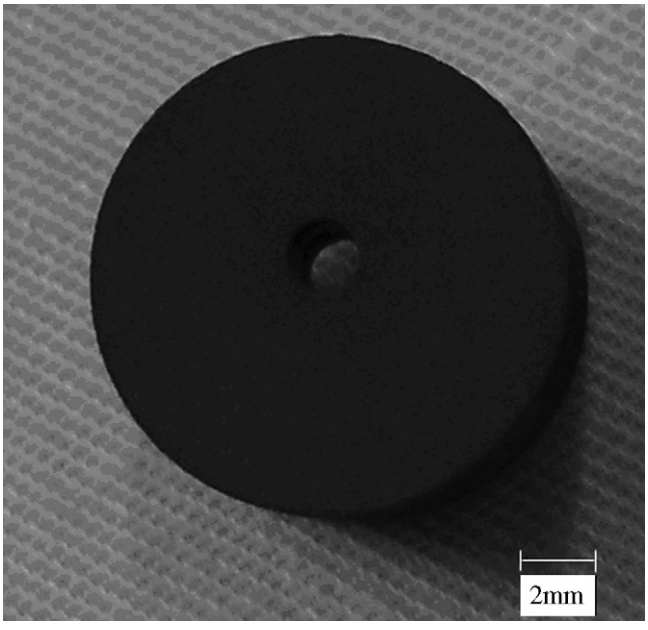

Fig. 3. Demonstration of the prepared machinable ZrB_2–SiC–BN ceramic composite using cemented carbide drill.

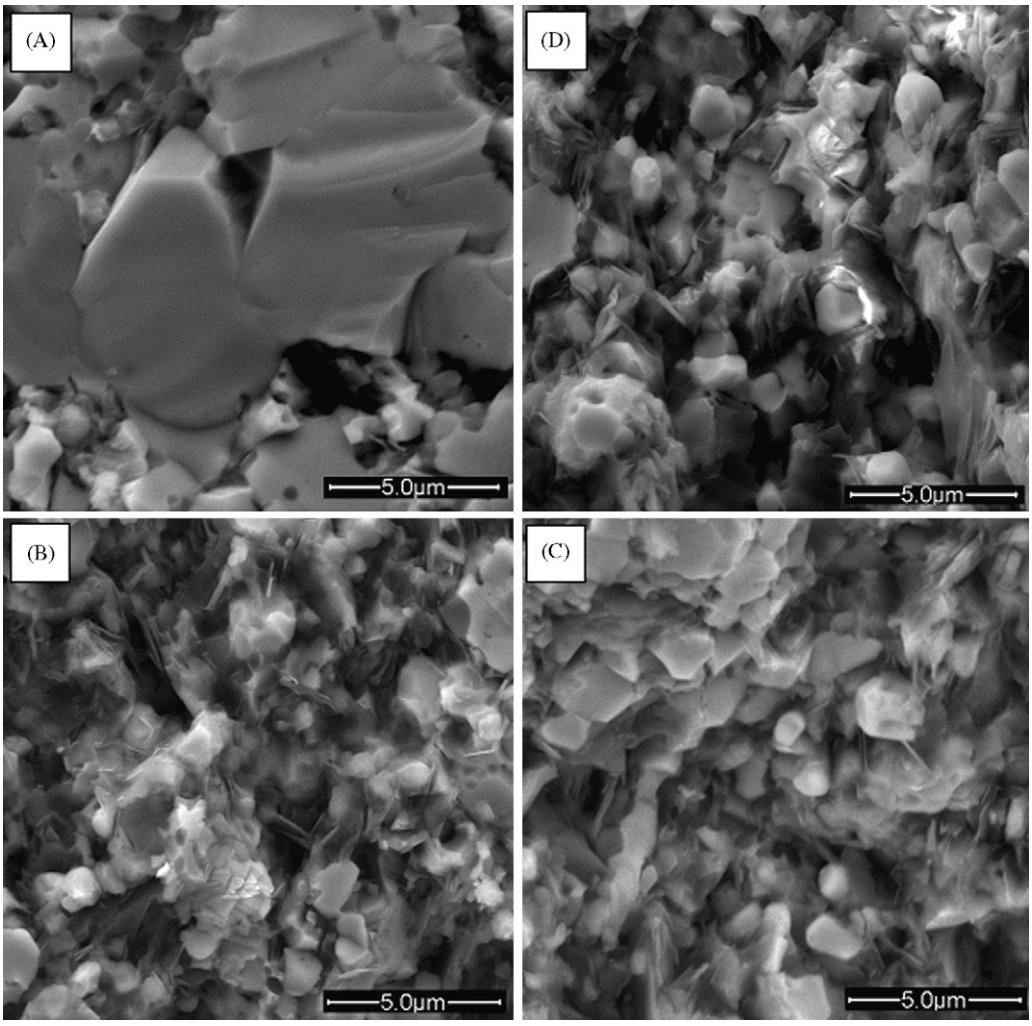

Fig. 4. SEM micrographs of the fracture cross-sections of samples ZS0 (A), ZS1 (B), ZS2(C) and ZS3 (D).

1100 °C and no significant weight gain was observed for the four specimens. While the weight gain rates of all the four samples increase abruptly as the temperature is up to 1500 °C, which indicates an accelerated oxidation. Moreover, the weight gain rate of ZS0 is the fastest among the four samples. During the isothermal oxidation stage at 1500 °C, the weight gain rate slows down compared to those during heating up or anisothermal stage from 1100 to 1500 °C, which results from the formation of oxide films on the surfaces. The formed oxide film actually acts as a barrier for further diffusion of oxygen into the fresh interface of ZrB_2–SiC–BN. It is interesting that the addition of BN restrains the oxidation during not only heating up stage but also the high temperature isothermal oxidation stage (1500 °C for 120 min), especially for ZS1 and ZS2 with medium contents of BN.

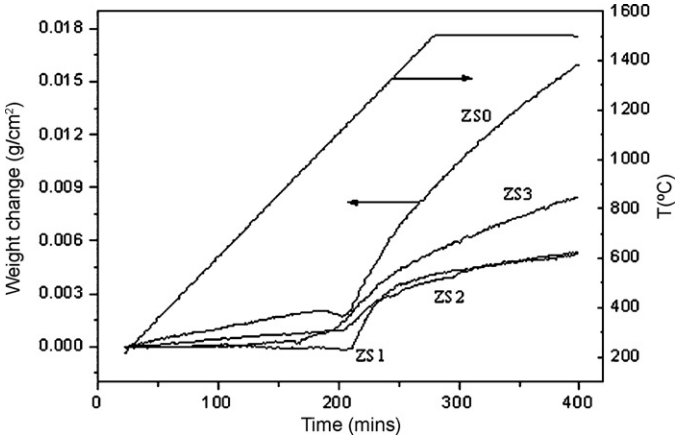

Fig. 5. TGA oxidation of ZrB_2 based composites in air up to 1500 °C.

3.2.2. Oxidation resistance of the composites in static air environment

The isothermal oxidation resistances for all the specimens were studied at 1100, 1300 and 1500 °C. The specific weight changes versus oxidation time are given in Fig. 6a–c. In general, the weight gain rates of all samples increase with the temperature and the specific weight change with time basically follows a parabolic oxidation law. The latter implies that the oxidation kinetics is controlled by transport of oxidant through the growing oxide film.

At 1100 °C, the sample ZS3 containing 35 vol%BN presents the highest rate of specific weight gain. However, minimum

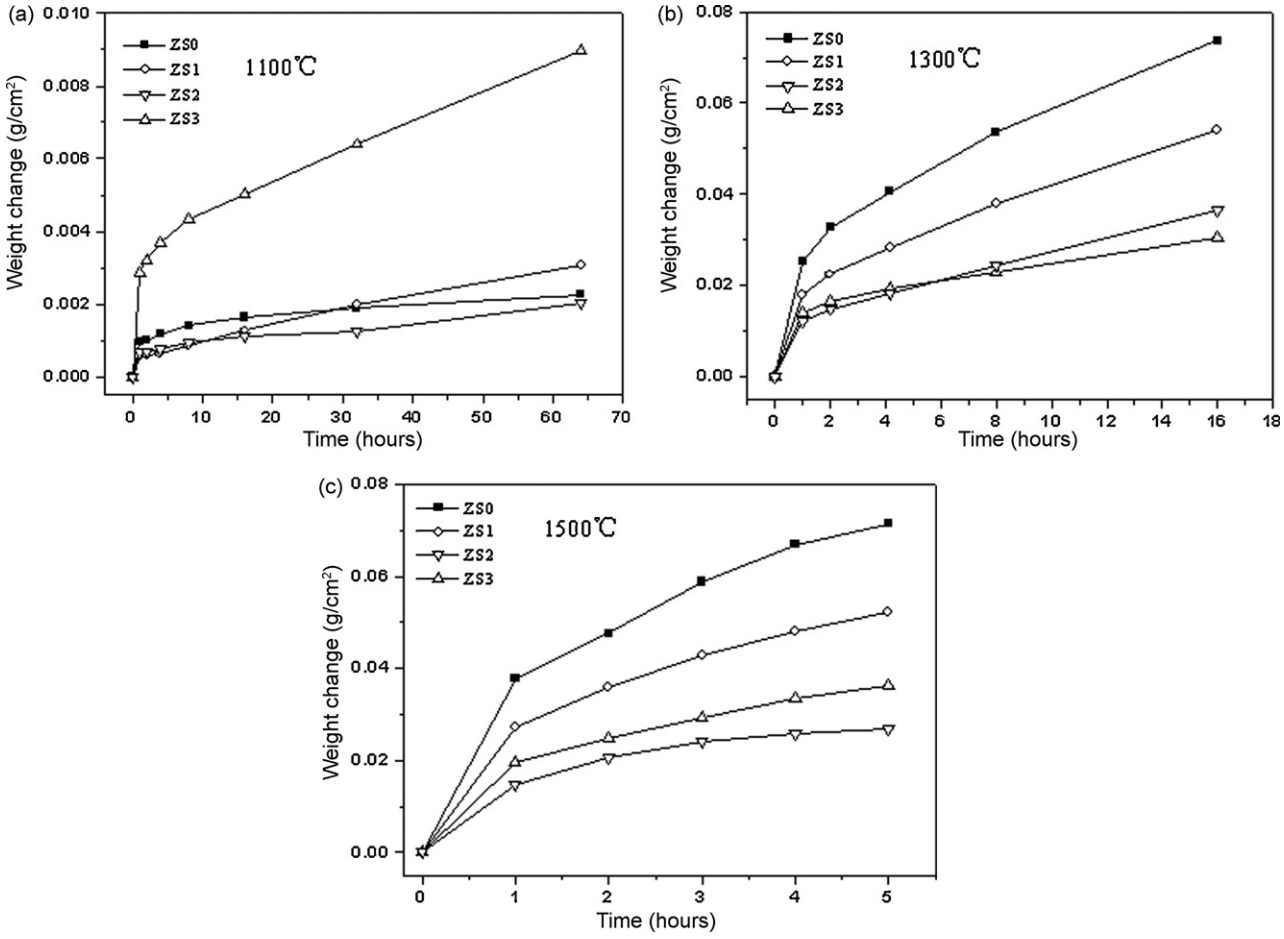

Fig. 6. Weight change of composites at (A) 1100 °C, (B) 1300 °C and (C) 1500 °C.

specific weight gain after 64 h, 0.0020 g/cm^2, was obtained for ZS2 (43.1%ZrB_2 + 26.9%SiC + 30%BN), which is slightly lower than that of ZS0 (80%ZrB_2 + 20%SiC), 0.0023 g/cm^2. At 1300 and 1500 °C, the highest rate of specific weight gain is ZS0, and ZS2 presents the lowest oxidation rate. The weight gain for ZS0 and ZS2 after oxidation at 1500 °C for 5 h were 0.0714 and 0.0268 g/cm^2, respectively. Therefore, it is concluded that the specimen ZS2 exhibits the best oxidation resistance from 1100 to 1500 °C.

For the modified composites, the expected main reactions describing the oxidation process are as follows:

$$2ZrB_2(s) + 5O_2(g) = 2ZrO_2(s) + 2B_2O_3(l) \quad (1)$$

$$2SiC(s) + 3O_2(g) = 2SiO_2(s) + 2CO(g) \quad (2)$$

$$4BN(s) + 3O_2(g) = 2B_2O_3(l) + 2N_2(g) \quad (3)$$

$$B_2O_3(l) = B_2O_3(g) \quad (4)$$

$$SiO_2(s) + xB_2O_3(l) = B_2O_3{\cdot}xSiO_2(l) \quad (5)$$

$$B_2O_3{\cdot}xSiO_2(l) = B_2O_3(g) + xSiO_2(s) \quad (6)$$

The reaction (1)–(3) lead to weight gains, and the reactions (4) and (6) lead to weight loss. The weight change of sample is accumulative results of reactions (1)–(4) and (6). The overall processes of oxidation may proceed through the following steps:

(a) *At the temperature from 600 °C to 1100 °C*. The generated liquid B_2O_3 would heal the cracks in the oxide scale, leading to the partially or completely sealing of the cracks depending on the formation rate of B_2O_3 from the reaction (1) and (3) and the viscosity of B_2O_3 liquid.[16]

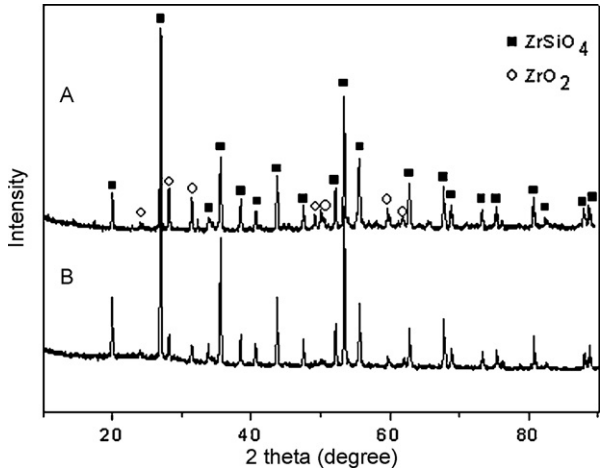

Fig. 7. XRD patterns of ZS0 (A) and ZS2 (B) oxidized at 1500 °C for 1 h.

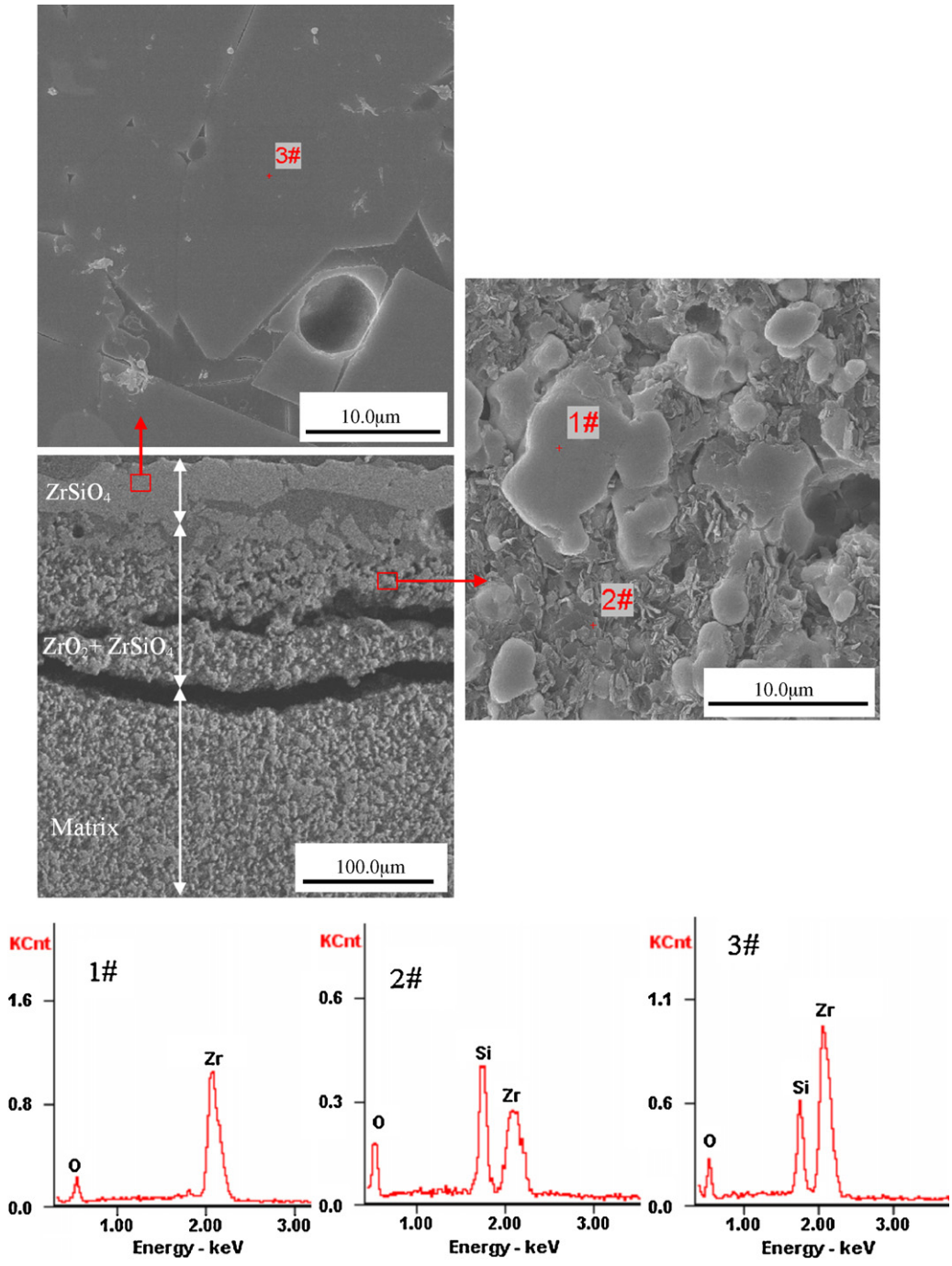

Fig. 8. Cross-sectional micrographs of ZS2 after oxidation at 1500 °C for 2 h.

(b) *During the temperature from 1100 °C to 1300 °C.* Large amount of volatile B_2O_3 would form. And very important, the formation of SiO_2 derived from the oxidation of SiC becomes significant, reaction between SiO_2 and B_2O_3 leads to a stable borosilicate glass. The borosilicates would act as a protective layer to reduce oxidation rate more effectively than B_2O_3 due to lower volatility and smaller oxygen diffusivity.[17–19] The sample ZS3 gets the highest rate of specific weight gain, which is attributed to the largest content of BN (35 vol%). The formation of B_2O_3 from the oxidation of BN shows the obvious weight gain. For the sample ZS2, it contains an appropriate amount of BN (30 vol%) compared with the sample ZS0, so more B_2O_3 was generated, and more easily spread in the material surface for oxide film. Moreover, the sample ZS2 contains a higher proportion of silicon carbide than ZS0 and ZS1, therefore more silicon oxide forms in ZS2 than that does in ZS0 and ZS1. The higher SiO_2 content in borosilicate glass, the higher the viscosity and melting point of borosilicate glass are, which can more effectively cover and protect the surface of samples. Therefore, the oxidation resistance of ZS2 with a suitable amount of BN additive is better than other samples.

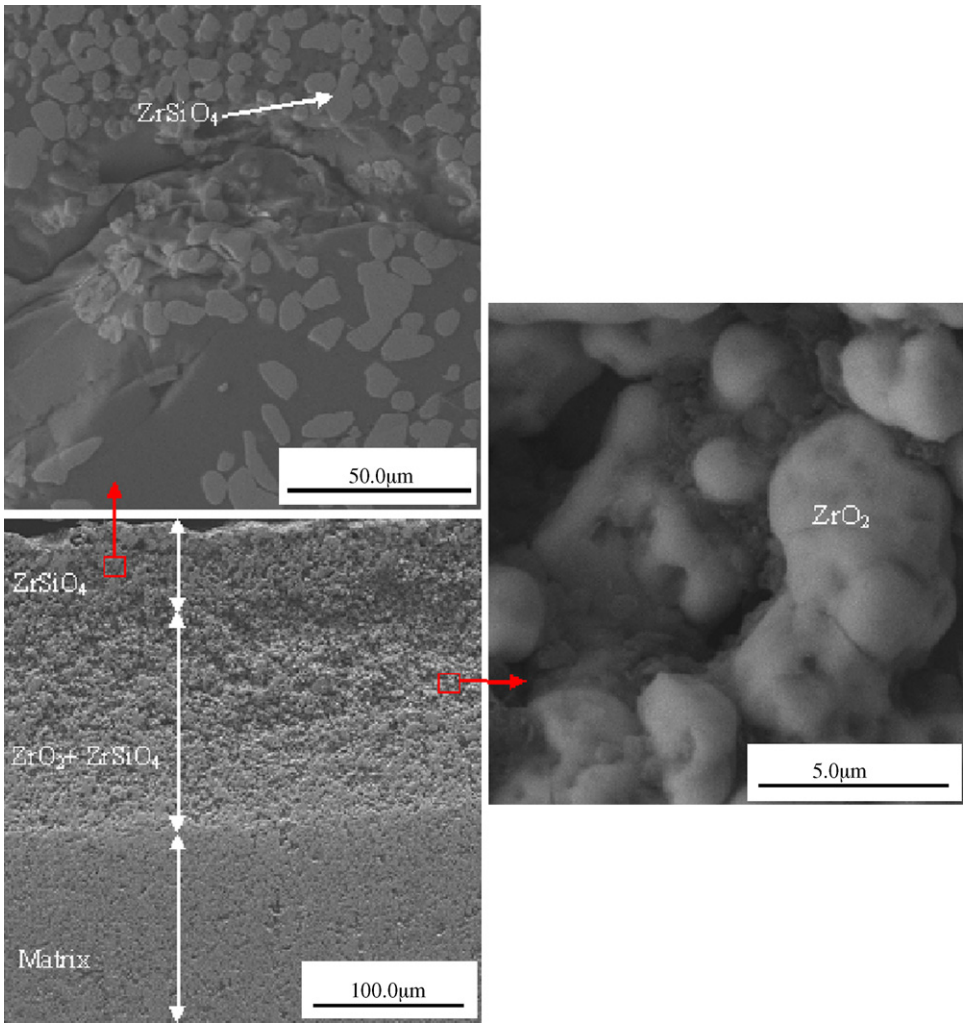

Fig. 9. Cross-sectional micrographs of ZS0 after oxidation at 1500 °C for 2 h.

(c) *With increasing temperature, 1300–1500 °C.* The viscosity of borosilicate glass decreases with increasing temperature, which benefits a healing of cracks and the diffusion velocity of oxygen. When temperature is up to 1500 °C, the initially formed silica-enriched glass will be gradually lost in response to the reaction (6) due to the substantive volatilization of B_2O_3. While SiO_2 is significantly less volatile than B_2O_3 at these temperatures (the vapor pressure of B_2O_3 is 10^5 times higher than that of SiO_2 at 1500 °C),[20] the remaining silicon oxide may react with zirconium oxide to generate a new anti-oxidation coating, zirconium silicate, which was confirmed by phase analysis in the study for the first time.

Fig. 7 shows the XRD patterns of the surface coatings of ZS2 and ZS0 oxidized at 1500 °C for 1 h. Monoclinic ZrO_2 and tetragonal $ZrSiO_4$ were observed. Since the B_2O_3 and borosilicate are amorphous, some undetected B_2O_3 probably may remain dissolved in the SiO_2. The presence of $ZrSiO_4$, presumably derived from the chemical reaction between ZrO_2 and SiO_2 (reaction (7)), stabilizes SiO_2 and inhibits the volatilization of silica. Besides these, $ZrSiO_4$ has high melting point and viscosity, it can efficaciously cover the sample surface and seal the cracks, which effectively limits the inward transport of oxygen and correspondingly enhances the resistance to oxidation.

$$ZrO_2 + SiO_2 = ZrSiO_4 \quad (7)$$

Figs. 8 and 9 show SEM results for the oxidized ZS0 and ZS2 after oxidation at 1500 °C for 2 h, respectively. It is noticeable that the oxide scales of both ZS0 and ZS2 consist of two distinct layers and the oxide layer of the specimen ZS0 (214 μm) is thicker than that of ZS2 (169 μm), which also indicates that the oxidation resistance of ZS2 is better than that of ZS0. The outer layers of both them are identified as $ZrSiO_4$, according to the combination of the EDS and XRD. In the inner layer, it is observed that white zirconia particles as a skeleton distribute in grayer zirconium silicate. The ZrO_2 does not enhance the oxidation protection, but may provide mechanical integrity and strength like a framework for the liquid glass. At the same time, cracks were found in oxide layer during the quenching process, which attributes to the coefficients of thermal expansion mismatch between the oxide layer and matrix.

EDS shows that zirconium, oxygen and silicon are present as the primary elements in the oxidized layer. Although quantitative

analysis for B is not possible by EDS since B is beyond the limit of the detection capability, a small amount of B element may still exist as borosilicate, though a previous SIMS investigation showed the amount being minimal.[20]

It is worth noting that the outer layer of ZS2 appears compact and adherent, while that of ZS0 is discontinuous and incompact. Furthermore, the thickness of ZS2 is remarkably lower than that of ZS0. This is due to the fact that the formation of this layer is mostly dependent on the SiC content. The silicon carbide content of ZS2 is higher than that of ZS0. A high SiC content is beneficial for the formation of $ZrSiO_4$, which can act as an effective barrier against the inward diffusion of oxygen.

4. Conclusions

(1) ZrB_2–SiC–BN ceramics were successfully prepared by hot-pressing under argon at 1800 °C and 23 MPa pressure. With the addition of BN, the flexural strength of the ZrB_2–SiC composite was improved, and the fracture toughness decreased slightly, but the hardness decreased enormously, and the machinability of this composite was improved noticeably.

(2) Below 1300 °C, the addition of BN significantly improved the oxidation resistance of ZrB_2–SiC ceramics due to the formation of ample borosilicates. At 1300 °C and above, zirconium silicate deriving from the reaction between silica and zirconium oxide played as a major anti-oxidation coating, which could inhibit the diffusion of oxygen and protect the material underneath from further oxidation after evaporating of borosilicates.

(3) The composite with components of 43.1%ZrB_2, 26.9%SiC and 30%BN showed excellent oxidation resistance up to 1500 °C. A total weight gain as low as 0.0268 g/cm^2 after oxidation at 1500 °C for 5 h was observed. The addition of BN in the appropriate amount is implied as an effective method to simultaneously improve the flexural strength, machinability and the oxidation resistance of ZrB_2–SiC ceramics.

Acknowledgements

Financial support from the Chinese Academy of Sciences under the Program for GF Basic Research (No. A1320070102) is gratefully appreciated.

References

1. Zimmermann, J. W., Hilmas, G. E., Fahrenholtz, W. G., Monteverde, F. and Bellosi, A., Fabrication and properties of reactively hot pressed ZrB_2–SiC ceramics. *J. Eur. Ceram. Soc.*, 2007, **27**, 2729–2736.
2. Levine, S. R., Opila, E. J., Halbig, M. C., Kiser, J. D., Singh, M. and Salem, J. A., Evaluation of ultra-high temperature ceramics for aeropropulsion use. *J. Eur. Ceram. Soc.*, 2002, **22**, 2757–2767.
3. Zhou, X. J., Zhang, G. J., Li, Y. G., Kan, Y. M. and Wang, P. L., Hot pressed ZrB_2–SiC–C ultra high temperature ceramics with polycarbosilane as a precursor. *Mater. Lett.*, 2007, **61**, 960–963.
4. Monteverde, F., Bellosi, A. and Scatteia, L., Processing and properties of ultra-high temperature ceramics for space applications. *Mater. Sci. Eng. A*, 2008, **485**, 415–421.
5. Yang, F. Y., Zhang, X. H., Han, J. C. and Du, S. Y., Characterization of hot-pressed short carbon fiber reinforced ZrB_2–SiC ultra-high temperature ceramic composites. *J. Alloys Compd.*, 2009, **472**, 395–399.
6. Zhang, W. Y. and Gao, H., Microstructures, properties and fabrication of machinable ceramics. *J. Synth. Cryst.*, 2005, **34**, 170–173.
7. Wang, R. G., Pan, W., Jiang, M. N., Chen, J., Luo, Y. M. and Sun, R. F., Development in machinable ceramics and machining technology of engineering ceramics. *Bull. Chin. Ceram. Soc.*, 2001, **3**, 27–35.
8. Xu, H. H. K. and Jahanmir, S S, Scratching and grinding of a machinable glass-ceramic with weak interfaces and rising T-curve. *J. Am. Ceram. Soc.*, 1995, **78**, 497–500.
9. Zhang, G. J., Yang, J. F., Ando, M. and Ohji, T., Nonoxide–boron nitride composites: in situ synthesis, microstructure and properties. *J. Eur. Ceram. Soc.*, 2002, **22**, 2251–2254.
10. Cho, M. W., Kim, D. W. and Cho, W. S., Analysis of micro-machining characteristics of Si_3N_4–hBN composites. *J. Eur. Ceram. Soc.*, 2007, **27**, 1259–1265.
11. Li, Y. L., Zhang, J. X., Qiao, G. J. and Jin, Z. H., Fabrication and properties of machinable 3Y–ZrO_2/BN nanocomposites. *Mater. Sci. Eng. A*, 2005, **397**, 35–40.
12. Kusunose, T., Sekino, T., Choa, Y. H. and Niihara, K., Fabrication and microstructure of silicon nitride/boron nitride nanocomposites. *J. Am. Ceram. Soc.*, 2002, **85**, 2678–2688.
13. Wang, R. G., Pan, W., Chen, J., Jiang, M. N. and Fang, M. H., Fabrication and characterization of machinable Si_3N_4/h-BN functionally graded materials. *Mater. Res. Bull.*, 2002, **37**, 1269–1277.
14. Li, Y. L., Qiao, G. J. and Jin, Z. H., Machinable Al_2O_3/BN composite ceramics with strong mechanical properties. *Mater. Res. Bull.*, 2002, **37**, 1401–1409.
15. Wang, X. D., Qiao, G. J. and Jin, Z. H., Fabrication of machinable silicon carbide–boron nitride ceramic nanocomposites. *J. Am. Ceram. Soc.*, 2004, **87**, 565–570.
16. Naslain, R., Design, preparation and properties of non-oxide CMCs for application in engines and nuclear reactors: an overview. *Compos. Sci. Technol.*, 2004, **64**, 155–170.
17. Jacobson, N. S. and Morscher, G. N., High-temperature oxidation of boron nitride: ii. Boron nitride layers in composites. *J. Am. Ceram. Soc.*, 1999, **82**, 1473–1482.
18. Baskaran, S. and Halloran, J. W., Fibrous monolithic ceramics: III. mechanical properties and oxidation behavior of the silicon carbide/boron nitride system. *J. Am. Ceram. Soc.*, 1994, **77**, 1249–1255.
19. Guo, Q. G., Song, J. R., Liu, L. and Zhang, B. J., Relationship between oxidation resistance and structure of B_4C–SiC/C composites with self-healing properties. *Carbon*, 1999, **37**, 33–40.
20. Rezaie, A., Fahrenholtz, W. G. and Hilmas, G. E., Oxidation of zirconium diboride–silicon carbide at 1500 °C at a low partial pressure of oxygen. *J. Am. Ceram. Soc.*, 2006, **89**, 3240–3245.